

Preparation and characterization of U₃O₈ nanoparticles via solid –state thermal decomposition of a new dioxidouranium (VI) complex [UO₂(L)(DMF)]: L= 2, 2'-((1E, 1E')-(1, 2 phenylen bis (azanylylidene)) bis (methanylylidene)) bis (4-bromo phenol)

Zeinab Tohidiyan^a, Iran Sheikhshoae^{a*}, Moj Khaleghi^b

^aDepartment of Chemistry, Shahid Bahonar University of Kerman, Kerman, Iran

^bDepartment of Biology, Shahid Bahonar University of Kerman, Kerman, Iran

Article history:

Received: 18/Dec/2015

Received in revised form: 18/Feb/2015

Accepted: 28/Feb/2016

Abstract

A new uranyl Schiff base complex, [UO₂(L)(DMF)] where L= 2, 2'-((1E, 1E')-(1, 2 phenylen bis (azanylylidene)) bis (methanylylidene)) bis (4-bromo phenol) by reaction between of H₂L and (CH₃COO)₂UO₂·2H₂O was successfully synthesized. The complex characterized by FT-IR, ¹H NMR as well as electronic and luminescence property measurements. This complex was used as a novel precursor for preparing U₃O₈ nanopowder at low temperature (400 °C) by decomposition method. The average crystallite size of the U₃O₈ nanopowder that has been synthesized is about 22. nm as determined by the Scherrer equation. According the results, we found that U₃O₈ could stop biofilm formation in *S. aureus* PTCC 1112 (0.632 mg/ml), *M. luteus* PTCC 1110 (0.633 mg/ml) and *E. faecalis* (0.633 mg/ml). Also, U₃O₈ repressed biofilm formation in *M. luteus* PTCC 1110 (0.625 mg/ml), *E. faecalis* (0.313 mg/ml) and *C. albicans* PTCC 5027 bacterias (1.27 mg/ml).

Keywords: Nanoparticle, U₃O₈, XRD pattern, Uranyl complex, luminescence, Antibacterial.

*. **Corresponding Author:** Department of Chemistry, Faculty of Science, Shahid Bahonar University of Kerman, Kerman, Iran, E-mail address: shoae@uk.ac.ir; i_shoae@yahoo.com; Tel. & Fax: +98 3132 2143

1. Introduction

Nowadays, the uranyl compounds for reduction of nuclear waste generated along with the extraction of uranium from sea and soil has been the subject of many investigations in environmental field [1-3]. Uranium is an important nuclear fuel due to the complexity of atomic structure and the abundance of energy levels [4]. Uranium dioxide is widely used as nuclear fuel in light water reactors due to important uranium–oxygen systems. They are prepared by calcination (thermal decomposition) of the ammonium uranyl carbonate to triuranium octaoxide, followed by reduction to uranium dioxide using cracked ammonia at about 700 °C [5]. The process optimization and preparation of U₃O₈ by calcination from ammonium uranyl carbonate in microwave fields were study by a Chinese group [6]. Also uranyl compounds with Schiff base complexes occupy an important role in the development of coordination chemistry due to the interesting properties, such as selective ion-exchange [7], mixed valency [8], electrical conductivity [9], enhanced fluorescence [10], and non-linear optical [11] properties. The uranyl compounds can exhibit catalytic, biological and sensor applications [12-14].

Other stable compounds of uranium are uranium oxides such as UO₂, UO₃ and U₃O₈ and so on. Among of them, U₃O₈ have the most stable in oxidizing atmosphere, that as the “yellow cake” produced by refining uranium ore [15]. Furthermore, U₃O₈ is applied in electrochemical [16] and catalyst [17] fields.

Hence, preparation of uranium compounds, including Schiff base complexes and uranium oxides is the best way for preventing of issues of uranium metal in environment meanwhile converted into useful materials.

As, synthesis of materials in nano scale has been increasing based on the fact that the reduction in particle size to nanometer scale results fascinating physical and chemical properties such as the mechanical, optical, and magnetic properties that are different from the bulk analogues [18, 19]. In this paper, we succeeded in preparing a new uranyl Schiff base complex, dimethyle

formamide - 2, 2'-((1E, 1E')-(1, 2 phenylen bis (azanylylidene)) bis (methanylylidene)) bis (4-bromo phenolato dioxidouranium (VI) complex and it was used as a new precursor for preparing U₃O₈ nano powder at low temperature by decomposition method.

The structure, spectral characterization of newly synthesized uranyl complex precursor was investigated by means of Fourier transformed infrared (FT-IR), Nuclear magnetic resonance (¹H NMR), as well as electronic and luminescence property measurements. Solid-state structure of the compound was confirmed by X-ray crystallography. The average crystallite size of the U₃O₈ powder was obtained from thermal decomposition of this complex is about 3 nm as determined by the Scherrer equation by using data of the X-ray diffraction (XRD).

2. Experimental procedure

2. 1. Materials and Methods

All the chemical reagents used in experiments were of spectroscopic grade and used as received without further purification. Fourier transform infrared (FT-IR) spectra were recorded on a Shimadzu system FT-IR 8400 spectrophotometer using KBr pellets. Nuclear magnetic resonance spectra were recorded on Bruker Avance-400 MHz. spectrometer. ¹H NMR chemical shifts were reported using tetramethylsilane (TMS) as the internal standard. Melting points were measured on an Electrothermal 9100 apparatus. Product X-ray diffraction (XRD) data was recorded by a Rigaku D-max C III, X-ray diffract meter using Ni-filtered Cu K α radiation. Electronic spectra of the complexes were recorded at 3 \times 10⁻⁵ mol L⁻¹ in EtOH solution using Cary 50 spectrophotometer in the 280–780 nm range. Fluorescence experiment was carried out on a Cary Eclipse spectro fluorometer from 400–600 nm at room temperature.

2.2. Synthesis of 2, 2'-((1E, 1E')-(1, 2 phenylen bis (azanylylidene)) bis (methanylylidene)) bis (4-bromo phenol): (H₂L)

H₂L was synthesis according to the literature [20], a methanolic solution of 1, 2-diaminobanzene (0.5 g,

0.002 mmol) was added drop wise to a methanolic solution of 5-bromosalicylaldehyde (0.4 g, 0.004 mmol) with constant stirring at room temperature; the formed precipitate was separated by filtration, and washed successively with cold methanol, and dried under vacuum over anhydrous CaCl_2 . Orange's crystals were obtained by slow evaporation from mother liquor for several hours, M.p: 190 °C.

2.3. Synthesis of dimethyle formamide - 2, 2'-((1E, 1E')-(1, 2 phenylen bis (azanylylidene)) bis (methanylylidene)) bis (4-bromo phenolato dioxidouranium (VI) complex [UO₂(L)(DMF)]

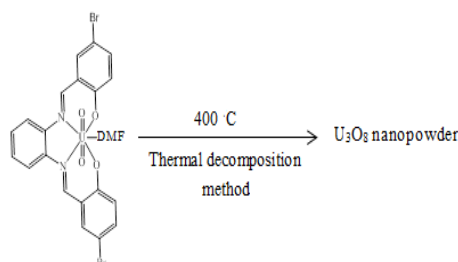
A DMF solution of (H_2L) (0.15 g, 0.0003 mol in 10 mL DMF) was added dropwise to a DMF solution of $(\text{CH}_3\text{COO})_2\text{UO}_2 \cdot 2\text{H}_2\text{O}$ (0.14 g, 0.0003 mmol in 3 mL DMF) with constant stirring. The mixture was refluxed for 1 h. The orange solution was obtained. Appropriate pure crystals were obtained from this solution by slow evaporation for several days.

M.p.> 300°C, Yield: 60%. Anal. Calc. for $\text{C}_{23}\text{H}_{18}\text{Br}_2\text{N}_2\text{O}_5\text{U}$ (800.20 g mol⁻¹): C, 34.49; H, 2.24; N, 3.49%. Found: C, 34.57; H, 2.35; N, 3.58%. FT-IR (KBr) cm⁻¹: $\nu(\text{CH})$ 2923–3447w; $\nu(\text{C}=\text{N}) + \nu(\text{C}=\text{C})$ 1607vs, 1580s; $\nu(\text{C}=\text{C})$ 1445s, 1409m; $\nu(\text{CO})$ 1162 m; $\nu(\text{N}=\text{C}-\text{N})$ 1234m; $\nu_{\text{asy}}(\text{trans}-\text{UO}_2)$ 943s; $\nu_{\text{sy}}(\text{trans}-\text{UO}_2)$ 896s; $\delta_{\text{oopb}}(\text{CH})_{\text{aromatic}}$ 742m. ¹H NMR (400 MHz, DMSO-d₆): δ = 9.5 (s, 1H, CH=N), 8.0–6.9 (m, 6H, aromatic protons), 3.3 (s, 6H, CH₃, DMF), 2.4–2.8 (s, 6H, DMSO). UV/Vis (ethanol) λ_{max} nm (log ϵ , LM⁻¹ cm⁻¹): 293 (6.86), 352 (6.94), 429 (7.03), 583 (7.16).

2.4. Synthesis of nanosized U₃O₈

To prepare U₃O₈ nanopowder, 1 g of the dimethyle formamide - 2, 2'-((1E, 1E')-(1, 2 phenylen bis (azanylylidene)) bis (methanylylidene)) bis (4-bromo phenolato dioxidouranium (VI) complex [UO₂(L)(DMF)] precursor complex was loaded into a porcelain crucible and then was placed in oven and heated at a rate of 2 °C min⁻¹ from room temperature to 400 °C in air and was maintained at 400 °C for 1 h (Scheme 1). The decomposition product generated from the complex was cooled to room temperature and

washed with DMF for at least three times and two times with EtOH to remove impurities, if any, and dried at room temperature for two days. The pure product of nano powders was characterized by XRD techniques.



Scheme 1. Synthesis of nano sized U₃O₈ and dimethyle formamide - 2, 2'-((1E, 1E')-(1, 2 phenylen bis (azanylylidene)) bis (methanylylidene)) bis (4-bromo phenolato dioxidouranium (VI) complex [UO₂(L)(DMF)] as a precursor

3. Results and discussion

Dimethyle formamide - 2, 2'-((1E, 1E')-(1, 2 phenylen bis (azanylylidene)) bis (methanylylidene)) bis (4-bromo phenolato) dioxidouranium (VI) complex [UO₂(L)(DMF)] complex was synthesized by the usual heating method. Uranium oxide (U₃O₈) in nano scale was prepared by thermal decomposition method. This method is simple, safe, low-cost and having easy experimental procedure.

The infrared spectrum of the [UO₂(L)(DMF)] complex where L= 2, 2'-((1E, 1E')-(1, 2 phenylen bis (azanylylidene)) bis (methanylylidene)) bis (4-bromo phenol) is shown in Fig. 2. The red shift of $\nu(\text{C}=\text{N})$ from 1628 cm⁻¹ in the IR spectrum of the H₂L to the 1607 cm⁻¹ regions of the IR spectrum of the complex and absence the stretching vibration of the phenolic OH suggests the coordination of the azomethinic nitrogens and phenolic oxygens to the metal centers. The various vibrations $\nu(\text{U}-\text{N})$ and $\nu(\text{U}-\text{O})$ in the complex are assigned to bands occurring in 632, 534 cm⁻¹, respectively. The strong absorption bands at 896, 943 cm⁻¹ have been assigned to $\nu_{\text{symm}}(\text{UO}_2)$ and $\nu_{\text{asy}}(\text{UO}_2)$, respectively. Which the stretching frequency of O=U=O due to the number, and type of ligands bound in the uranyle equatorial plane [21–23].

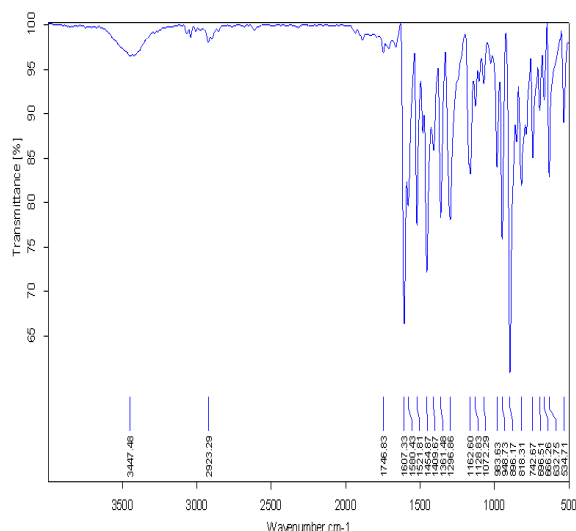


Figure 2. FT-IR spectrum of dioxidouranium (VI) complex $[UO_2(L)(DMF)]$

1H NMR spectrum of the dioxidouranium (VI) complex (Figure 3) was recorded in $DMSO-d_6$. The signal of the azomethinic proton of the complex is at lower field (downfield shielding) than the ligand. Also signal due to OH proton is not observed in the spectrum of the complex, indicating that the coordination takes place through nitrogen and oxygen to metal.

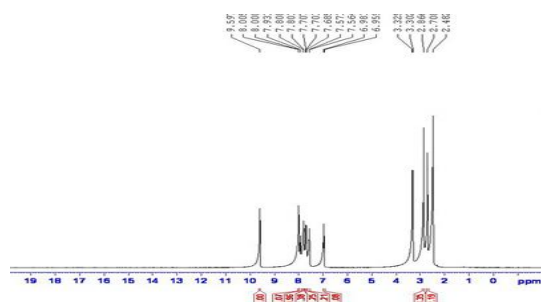


Figure 3. 1H NMR spectrum of $[UO_2(L)(DMF)]$ complex

The fluorescence spectrum (Figure 4) of dioxidouranium (VI) complex (2×10^{-5} mol L^{-1} in EtOH solution) is shown in Fig. 4. The emission band is located at 493 nm when excited at 350 nm. The fluorescent emission originates from the azomethine chromophore (C=N) to the metal charge transfer (LMCT) occurring between the 6d orbital of $U^{(VI)}$ and the ligand [18].

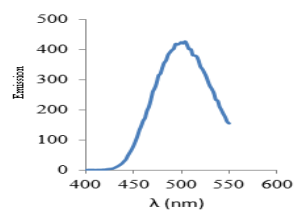


Figure 4. Fluorescence emission spectra of $[UO_2(L)(DMF)]$ complex (2×10^{-5} mol L^{-1} ; EtOH)

The electronic spectrum of dioxidouranium (VI) complex was recorded in EtOH solution from 280–780 nm (Figure 5). The electronic spectrum shows the band at 293 nm is attributed to $\pi \rightarrow \pi^*$ transitions associated with the phenyl rings and the band at about 352 nm arise from $\pi \rightarrow \pi^*$ transitions associated with the azomethine chromophore [3]. As uranyl complexes contain U (VI) has an empty valence shell, the metal center is only as an acceptor site for LMCT transitions. The charge transfer bands assigned to $N \rightarrow M$ and $O \rightarrow M$ electron transfer occur at in 429 nm and 583 nm respectively [24].

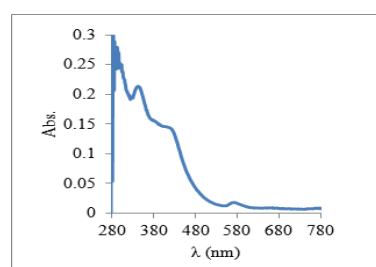


Figure 5. Electronic absorption spectrum of $[UO_2(L)(DMF)]$ complex (3×10^{-5} mol L^{-1} ; EtOH)

The XRD pattern of the decomposition product of the dioxidouranium (VI) complex $[UO_2(L)(DMF)]$ is shown in Fig. 6. The XRD pattern reveals only the diffraction peaks attributable to U_3O_8 with hexagonal (JCPDS Card No. 04-0511), and orthorhombic (JCPDS Card No. 47-1493) phases.

At ambient conditions, the U_3O_8 have an orthorhombic structure and it transforms to a hexagonal structure at elevated temperature (~ 350 °C) [15]. At temperatures higher than 875 °C, the structure of U_3O_8 changes continuously, the reason of it may be related to the loss of oxygen content. In this context, we describe the synthesis of U_3O_8 from decomposition of $[UO_2(L)(DMF)]$ complex where $L = 2, 2'-((1E, 1E)-(1, 2$ phenylen bis (azanylylidene)) bis (methanylylidene)) bis (4-bromo phenol) at 400 °C. In this condition, U_3O_8

was obtained with hexagonal and orthorhombic phases. However, the size, morphology, and structure of product prepared are strongly dependent on type of precursor and the synthetic methods.

No peaks of impurity were found in the XRD pattern, indicating that the nanocrystalline U_3O_8 obtained via this synthesis method consists of pure product. It can be seen from XRD pattern that the diffraction peaks are markedly broadened due to the small size effect of the particles. The average size of the U_3O_8 particles was estimated to be about 3 nm using diffraction peaks at $2\theta=21.49, 26.09, 34.04,$ and 51.80 by Scherrer equation 1 [25]. In the main phase the major peaks were indexed as (001), (130), (131) and (331). The average crystallite size was estimated by Scherrer equation using the most intense peak (130):

$$d = k \lambda / (\beta \cos \theta) \quad (\text{Equation 1})$$

Where d [nm] is the mean size of the crystalline domain (crystalline size) of the synthesized materials, k is the shape factor (dimensionless) which has the typical value of 0.9 (but depends on the shape of particles), λ [nm] is the X-ray wavelength, β [rad.] is the peak width at half of the maximum intensity (FWHM) and θ [rad] is the peak position (Bragg angle). $K=0.9$, and $\lambda=0.1541$ nm was used to calculate the mean crystalline size (d) of the U_3O_8 nano powder. Based on this equation, the average crystallite size was calculated as ~ 22.82 nm.

Figure 6 show the XRD pattern of the prepared U_3O_8 nanoparticles at 400°C .

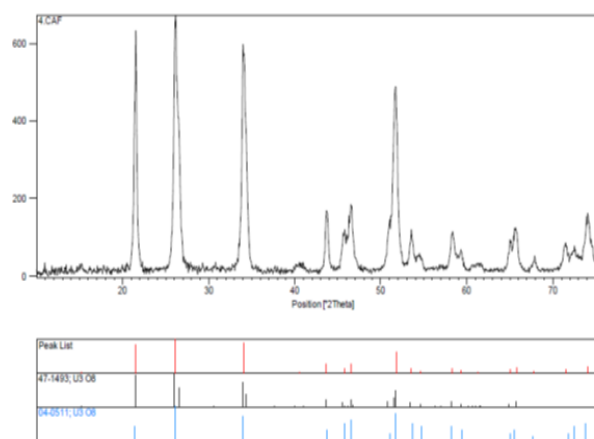


Figure 6. The XRD pattern of the synthesized nano sized U_3O_8 via a combustion method of $[UO_2(L)(DMF)]$ complex without fuel at 400°C .

3.2. Antibacterial assay

The antimicrobial activity of the synthesized U_3O_8 nanoparticles was tested *in vitro* against some microorganisms. Stock solution (1 mg/mL) of the synthesized compound was prepared by dissolving this compound in dimethyl sulfoxide (DMSO).

Biofilms are a major cause of human infections. The majority of hospital-acquired infections are due to biofilms because they can be life-threatening colonizers of biomedical devices. Indeed, a large proportion of nosocomial infections are related to the colonization of pathogens on the surface of implanted medical devices such as respirators, catheters (central venous, urinary), prosthetic heart valves, and orthopedic devices. If biofilm formation is stopped, we can control the spread of infection. Therefore, in this study we decided to investigate the effect of the U_3O_8 nanoparticles on bacterial biofilm formation. For investigation of anti biofilm effect of U_3O_8 . Microtiter plate adhesion assay was employed: Biofilm formation in this assay was determined by the method reported earlier [26]. In this study, a culture of the bacteria and yeast were grown overnight in the broth media. Then, the overnight cultures were diluted 1:100 into fresh medium for biofilm assays. $100 \mu\text{L}$ of the dilution was added on well in a 96 well dish. For quantitative assays, we typically use 4-8 replicate wells for each treatment. The microtiter plate was incubated for 24 hrs at 37°C . After incubation, cells were dumped out by turning the plate over and shaking out the liquid. Finally, the biofilms were stained by the 0.1% crystal violet. The microtiter plate was incubated at room temperature for 10-15 min. After that, the plate was rinsed 3-4 times with water and dried. Absorbance at 540 nm was read after solubilization of the dye with 95% ethanol and in an enzyme-linked immunosorbent assay (ELISA) plate reader. Data for biofilm formation of all strains were compared with the data for the negative control.

Staphylococcus aureus PTCC 1431 was used as positive control and the microbial medium without microorganism was used as negative control.

Table 1 shows anti-biofilm effect of U_3O_8 . According to the results, we found that U_3O_8 stopped biofilm formation in *S. aureus* PTCC 1112 (0.632 mg/ml), *M. luteus* PTCC 1110 (0.633 mg/ml) and *E. faecalis* (0.633 mg/ml). Also, U_3O_8 repressed biofilm formation in *M. luteus* PTCC 1110 (0.625 mg/ml), *E. faecalis* (0.313 mg/ml) and *C. albicans* PTCC 5027 (1.27 mg/ml).

Table 1. Comparison of Anti-biofilm formation effect and MIC of U_3O_8 , (mg/ml)

Microorganisms	Compounds	
	U_3O_8	
	ABF*	MIC
<i>S. aureus</i> PTCC 1112	0.632	1.25
<i>M. luteus</i> PTCC 1110	0.633	1.25
<i>B. cereus</i> PTCC 1015	ND**	0.625
<i>Listeria monocytogenes</i> *	ND	0.313
<i>E. faecalis</i> *	0.633	1.25
<i>C. albicans</i> PTCC 5027	ND	1.27
* Anti-biofilm formation effect ** Not Determined before minimum inhibitory concentration.		

4. Conclusion

A new $[UO_2(L)(DMF)]$ complex where L= 2, 2'-((1E, 1E')-(1, 2 phenylene bis (azanylylidene)) bis (methanylylidene)) bis (4-bromo phenol) and its nano oxide U_3O_8 were synthesized by rapid method and characterized by some physiochemical and spectroscopic methods, such as FT-IR, 1H NMR, UV-Vis and X-ray diffraction (XRD). U_3O_8 nanopowder was prepared from decomposition of this compound. The average crystallite size of U_3O_8 nanopowder is about 3 nm as determined by the Scherrer equation. The advantage of this method is simplicity, safety and low-cost. The antibacterial activity of U_3O_8 against some Gram positive bacteria strains (*E. faecalis* S. *aureus* PTCC1112, *M. luteus* PTCC 1110) and a fungal species (*C. albicans* PTCC5027) were assessed by evaluating the presence of inhibition zone, minimum inhibitory concentration (MIC) values. It was observed that U_3O_8 showed antibacterial effect (Table 1).

Acknowledgments

Authors are grateful to the Shahid Bahonar University of Kerman for financial support of this study.

References

- [1] R. K. Sinha and A. Kakodkar, *Nucl. Eng. Des.* 236 (2006) 683.
- [2] Z. Asadi and M.R. Shorkaei, *Spectrochim. Acta, Part A*, 105 (2013) 344.
- [3] A.M.R. Neiva, P.C.S. Carvalho, I.M.H.R. Antunes, M.M.V.G. Silva, A.C.T. Santos, M.M.S. Cabral Pinto and P.P. Cunha, *Journal of Geochemical Exploration*, 136 (2014)102.
- [4] Duan Yi, Xiang, Susan, T., Sudip and P. Koirala, *Analytica Chimica Acta*, 532 (2005) 47.
- [5] S. K. Sik, and K. W. Kang, *J. Nucl. Mater.*, 317 (2003) 204.
- [6] Liu Bing-Guo, Peng Jin-Hui, C. Srinivasakannan, Zhang Li-Bo, Hu Jin-Ming, Guo Sheng-Hui and Kong Dong-Cheng, *Annals of Nuclear Energy*, 85 (2015) 879.
- [7] T. Y. Shvareva, P. M. Almond and T. E. Albrecht-Schmitt, *J. Solid State Chem.*, 178 (2005) 499.
- [8] D. Fernando Back, G. Manzoni de Oliveira, L. Andre Fontana, A. Neves, B. Almeida Iglesias, T.Pacheco Camargo, P.k T. Campos and J. Pinto Vargas, *Inorg. Chim. Acta.*, 48 (2015) 163.
- [9] N.A. El-Ghamaz, M.A. Diab, A.Z. El-Sonbati and O.L. Salem, *Spectrochim. Acta, Part A*, 83 (2011) 61.
- [10] S. Scapolan, E. Ansoborlo, C. Moulin and C. Madic, *J. Alloys Compd.* 271 (1998)106.
- [11] V.V. Klepov, L. B. Serezhkina, A. V. Vologzhanina, D. V. Pushkin, O. A. Sergeeva, S. Yu. Stefanovich and V. N.

- Serezhkin, *Inorg. Chem. Commun.* 46 (2014)5.
- [12] Z. Ma, M. Sutradhar, A. V. Gurbanov, A. M. Maharramov, R. A. Aliyeva, F. S. Aliyeva, F. N. Bahmanova, V. Mardanov, F. M. Chyragov and K. T. Mahmudov, *Polyhedron*, 101 (2015)14.
- [13] S. M. El-Megharbel, N. M. El-Metwaly and M. S. Refat, *Spectrochim. Acta, Part A*, 149 (2015) 263.
- [14] V. Zare-Shahabadi and M. Akhond abd J.d. Tashkhourian and F. Abbasitabar, *Sensors and Actuators B*, 141 (2009)34.
- [15] F.X. Zhang, M. Lang, J.W. Wang, W.X. Li, K. Sun, V. Prakapenka and R.C. Ewing, *J. Solid State Chem.*, 213 (2014)110.
- [16] S.M. Jeong, H.S Shin, S.S. Hong , J.M. Hur , J.B. Do and H.S. Lee, *Electrochim. Acta*, 55 (2010)1749.
- [17] V. R. Choudhary and D. K. Dumbre, *Appl. Catal, A.*, 375 (2010)252.
- [18] I. Sheikhshoaie and Z. Tohidiyan, *Can. J. Basic Appl. Sci.*, 3 (2015)164.
- [19] M. Panahi-Kalamuei , M. Mousavi-Kamazani, M. Salavati-Niasari and S. M. Hosseinpour-Mashkani , *Ultrason Sonochem.*, 23 (2015)246.
- [20] S.Y. Ebrahimipour, I. Sheikhshoaie, J. Castro, M. Dušek, Z. Tohidiyan, V. Eigner and M. Khaleghie, *RSC Adv.*, 5 (2015) 95104.
- [21] S. K. Gupta, N. Sen and R. J. Butcher, *Polyhedron*, 71 (2014) 34.
- [22] Z. Asadi, M. Asadi, F. Dehghani Firuzabadi and M. Ranjkesh Shorkaei, *J. Ind. Eng. Chem.*, 20 (2014) 4227.
- [23] D.M.W. Anderson, L.J. Bellamy and R.L. Williams, *Spectrochim Acta.*, 12 (1958) 233.
- [24] A. Fasihizad, T. Barak, M. Ahmadi, M. Dusek and M. Pojarova, *J. Coord. Chem.* 67 (2014) 2160.
- [25] H. P. Klug and L. E. Alexander: X-ray Diffraction Procedures, 2nd Ed., Wiley, New York, 1964.
- [26] H. Kubota, S. Senda, N. Nomura, H. Tokuda and H. Uchiyama, *J. Biosci. Bioeng.*, 106 (2008)381.

